

Pair production of heavy charged gauge bosons in pp collisions at LHC

Ijaz Ahmed,^{1,*} Fazal Khaliq,^{2,†} M. U. Ashraf,^{3,‡} Taimoor Khurshid,^{4,§} and Jamil Muhammad^{5,¶}

¹*Federal Urdu University of Arts, Science and Technology, Islamabad Pakistan*

²*Riphah International University, Hajj Complex, I-14 Islamabad*

³*Centre for Cosmology, Particle Physics and Phenomenology (CP3) Université catholique de Louvain, Chemin du Cyclotron, 2, B-1348 Louvain-la-Neuve, Belgium*

⁴*International Islamic University, H-10, Islamabad Pakistan*

⁵*Sang-Ho College, and Department of Physics, Konkuk University, Seoul 05029, South Korea*

Abstract

Two oppositely charged new heavy gauge boson pair production at the Large Hadron Collider (LHC), is presented in this paper. These bosons are known as W' boson due to the reason that it is the heavy version of Standard Model's weak force carrier, the W boson. The production cross section and decay width in proton-proton (pp) collision at $\sqrt{s} = 8$ TeV are calculated for different masses and coupling strengths of W' . Efficiencies for different signal regions and branching ratios for different decay channels are computed. In this study, the pair production ($W'^+ W'^-$) is considered in emerging new physics as a result of pp collision at $\sqrt{s} = 8$ TeV at the LHC with final state containing two tau (τ) leptons and two neutrinos (each W' decay to τ and its neutrino). The event selection efficiency similar to the CMS experiment is used for the mass of W' to set lower limits for different coupling strengths of W' and, the obtained results are presented in this work. For heavy gauge bosons, when coupling strength is similar to that of Standard Model's W boson, the mass of W' below 445 GeV are excluded at a confidence level of 95%.

PACS numbers: 12.60

Keywords: heavy gauge boson, LHC, tau leptons, proton Collider

*Electronic address: Ijaz.ahmed@fuuast.edu.pk

†Electronic address: fazalkhaliq44@gmail.com

‡Electronic address: usman.ashraf@cern.ch

§Electronic address: taimoor.khurshid@iiu.edu.pk

¶Electronic address: mjamil@konkuk.ac.kr

I. INTRODUCTION

A new physics can be observed at TeV energy scale. The new scenario of physics is the finding of additional new heavy gauge bosons (W'^{\pm}, Z'). Many extensions of the standard model realize the existence of these additional gauge bosons. These bosons are the heavy version of weak vector gauge bosons of the standard model (SM). The properties of these bosons may be similar or not to that of the standard model weak bosons W which depends upon the underlying theory. The model that predict heavy W' bosons also contains Z' bosons generically, but this is not true in the reverse [1].

Different theories and models predict the existence of heavy charged gauge bosons(W'). The standard model W bosons, in theories with extra dimension, may propagate in extra dimension, and gives rise to heavy copies [2]. One approach is the little higgs models. These models predict the existence of W' bosons, with the idea that the higgs boson is a nambu-goldstone boson [3]. In Left Right Symmetric Model (LRSM) charged gauge boson may be realized in symmetric way that can be left, right or both-handed [4, 5, 6]

The detail of the model gives the difference in mass of W' and Z' bosons, hence the discovery of W' bosons is more probable than the discovery of Z' bosons. The property that differentiates standard model W and the new heavy charged gauge bosons is that it may couple to left-handed, right-handed or mixture of both fermions while standard model weak bosons only couple to left-handed fermions. The lagrangian that generally gives mathematical description of fermions interaction of W' bosons is described in [1].

$$L = \frac{V_{ij}}{2\sqrt{2}} \bar{f}_i \gamma_{\mu} (g'_R(1 + \gamma^5) + g'_L(1 - \gamma^5)) W'^{\mu} f_j + h.c \quad (1)$$

Where left-hand (right-hand) coupling constant is given by $g'_{L(R)}$ respectively. The $V_{i,j}$ is the 3×3 identity matrix for lepton and it represents CKM matrix for quarks. The left and right-handed chiral projection operators are given by $(1 \pm \gamma^5)$. In case when $g'_R = 0$ and $g'_L \neq 0$, then W' boson has purely left-hand coupling where it couple with both leptons and quarks, while when $g'_R \neq 0$ and $g'_L = 0$, then only W' boson wil have purely right-handed coupling but only with quarks. Since the right-handed neutrinos do not exist, so coupling of W' boson is restricted with the leptons including neutrinos or the neutrino mass must be much higher than W' bosons, which is also not possible as the neutrinos masses are confirmed lying at few electron volts.

II. SEARCH OF HEAVY GAUGE BOSONS (W')

Different signatures are used in many experiments to search for W' bosons. In ATLAS experiment W' bosons are considered to decay into lepton along with missing transverse energy from neutrinos [6], where it excludes W' masses less than 5.1 TeV in standard model conditions at 95% confidence level. This paper excludes two main searches that can be done for the heavy-charged gauge boson via direct and Indirect searches.

In the past, extensive work on heavy charged gauge boson is performed both phenomenologically as well as experimentally e.g., in Ref. [7] ATLAS collaboration studied single W' production at LHC $pp \rightarrow W' \rightarrow l\nu$ using 139 fb^{-1} data at $\sqrt{s} = 13$ TeV where ($l = e$ or $l = \mu$) are extracted in the model-independent searches. Similarly, CMS experiment [9] explored $pp \rightarrow W' \rightarrow tb$ channel, where an integrated luminosity 2.6 fb^{-1} at $\sqrt{s} = 13$ TeV is used and results provide the most stringent limits for right-handed W' bosons in the top and bottom quark decay channel. A few research articles [10–12] are also reported in which analysis is carried out either at $\sqrt{s} = 8$ TeV in $\tau\nu$ final state or at $\sqrt{s} = 14$ TeV in High Luminosity LHC (HL-LHC).

In current study, two oppositely charged heavy gauge (W') bosons are produced in pp collisions at $\sqrt{s} = 8$ TeV as shown in figure 1. The pair of heavy charged gauge bosons decayed to τ and its neutrino in pp collisions figure.caption.3. Since this energy is easily accessible at LHC and abundant of such particles are produced where it can decays into τ leptons and its neutrinos final state (each W' decays to one τ and its neutrino). Due to the presence of neutrino in the final state $g'_L \neq 0$. The efficiencies calculated by CMS collaboration [8] are used in our study to compare the required signal yields having standard model backgrounds. This makes us able to set lower limits on W' mass. The integrated luminosity used is 18.1 fb^{-1} and 19.6 fb^{-1} for two different channels.

Many experimental analyses propose left or right-handed W' in the direct searches for W' bosons production at hadron colliders. These bosons decay into leptons in the final state with standard model-like couplings. The decay of right-handed or left-handed bosons into right-handed neutrino is kinematically restricted to the conditions on mass of W' that is $m_{W'} > 786$ GeV [13–20]. This decay is forbidden if mass of the right-handed neutrino is greater than mass of W' bosons. In di-jet data, right-handed W' bosons are directly restricted by peak search only. The light quarks have larger coupling with W' until to reach the limit for mass of 420 GeV [21–23] as limited by the di-jet QCD background.

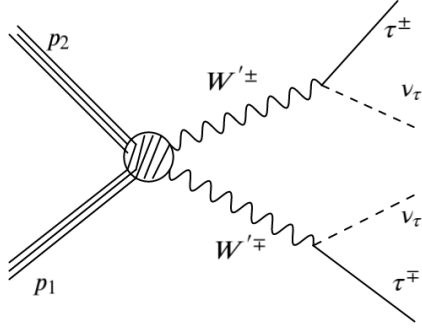


FIG. 1: The pair of heavy charged gauge bosons decayed to τ and its neutrino in pp collisions

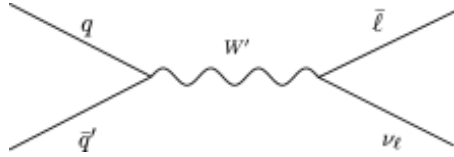


FIG. 2: W' production via quark anti-quark annihilation, and decays to lepton and its corresponding neutrino

W' boson can be detected directly at the LHC, by decaying to lepton and its neutrino or top and bottom quark in quark anti-quark annihilation is shown in figure 2 W' production via quark anti-quark annihilation, and decays to lepton and its corresponding neutrino figure.captio.4. This physics can be achieved at the energy scale of TeV.

A. Alternative search

The second method for the search of W' is the indirect method. The Standard Model W can be replaced by W' in some decay process like muon decay to set a limit on its mass for study. Figure 3A view of muon decay to electron and neutrinos figure.captio.6 presents a schemetic view of muon decay in which the SM W can be replaced in this process with the heavy charged gauge boson.

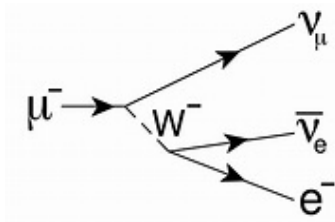


FIG. 3: A view of muon decay to electron and neutrinos

III. SIMULATION AND RESULTS

A. Cross section and decay width calculation

For the theoretical study of pair production of W' at $\sqrt{s} = 8$ TeV in pp collision and its decay into τ and its neutrino in the final state, Madgraph 2.6.0 [24] is used. It is the extension to Madgraph5 which is matrix-element generator. The events are generated in Madgraph, first considering only left-handed W' by setting the coupling parameter for W' ($g'_L = g_{SM}$, $g'_R = 0$) the interaction as permitted both to quarks and leptons. The mass of W' boson is varied from 110 GeV to 500 GeV with an increment of 30 GeV, selecting the total energy of beam 14 TeV (7 TeV for each beam of proton).

The decay width or lifetime was calculated using Madgraph for various masses and compared with the results in [1]. In this case the partial width for W' decays to $t\bar{b}$ and $\bar{t}b$ and the total decay width for W' in leading order and next to leading order precision is calculated. The results are in good agreement. The decay width is the function of modes of decay, process of decay, coupling constant which depend upon kinematics constraint. Estimation for production cross-section are also done by MadGraph. Decay width and production cross section for both quarks and leptons are given in table ICross section and decay width for different masses and different coupling constants.table.caption.9. The model does not keep the value of coupling constant fixed. Then we modified the coupling constant to find its effect on the production cross section and decay width, by increasing and decreasing (multiplying the left-hand coupling with 1.5 and 0.5 of the standard model) coupling constant. By this increase or decrease in coupling constant, cross-section also increases by factor of 5 and decreases by factor 0.062. The decay width increases or decreases by a factor of 2.25 and 0.25 respectively.

Now the left-handed and right-handed couplings are changed such that the sums of their square

are equal to the square of standard model coupling.

$$g_{SM}^2 = (g'_L)^2 + (g'_R)^2 \quad (2)$$

and

$$g'_L = g_{SM} \cos \theta \quad (3)$$

Where θ is the mixing angle, from the above equation it is observed that by changing angle from 0^0 to 90^0 , W' goes to purely right-handed from purely left-handed. The cross-section and decay width with different mixing angles for mass of $W' = 350$ GeV are given in Table II. The cross section and decay width for $m'_W = 350$ GeV for different mixing angles and branching ratios in $\tau\nu_\tau$ final state are given in Table III.

Mass (GeV)	$g'_R = 0, g'_L = 0.32$		$g'_R = 0, g'_L = 0.64$		$g'_R = 0, g'_L = 0.96$	
	$\sigma(pp \rightarrow W'^+ W'^-) (fb)$	$\Gamma(W' \rightarrow XY) (GeV)$	$\sigma(pp \rightarrow W'^+ W'^-) (fb)$	$\Gamma(W' \rightarrow XY) (GeV)$	$\sigma(pp \rightarrow W'^+ W'^-) (fb)$	$\Gamma(W' \rightarrow XY) (GeV)$
110	128.6	0.69	2055.3	2.8	10296.9	6.2
140	57.3	0.82	923.5	3.5	3950.8	7.9
170	22.4	1.1	360.1	4.3	1804.5	9.5
200	10.9	1.3	173.9	5.2	867.2	11.7
230	5.5	1.6	87.6	6.2	440	14
260	3.0	1.8	48	7.4	238	16.6
290	1.7	2.1	28.1	8.5	146.5	19.1
320	1.1	2.4	17.4	9.6	84.5	21.6
350	0.7	2.7	11.2	10.7	40.2	24.0
380	0.5	2.9	7.5	11.7	19.2	24.4
410	0.3	3.20	5.16	12.82	9.2	28.8
440	0.2	3.47	3.64	13.88	4.6	31.2
470	0.2	3.7	2.6	14.9	2.9	33.6
500	0.12	4.0	1.9	15.9	1.2	35.9

TABLE I: Cross section and decay width for different masses and different coupling constants.

B. Branching ratios

W' boson decay to different final states, in the current study we only consider τ and its neutrino in the final state. TAUOLA package [25] is used for the simulation of τ lepton decays. This package is also used for the leptonic and hadronic decay of taus, to simulate in the final state. It also gives full information of neutrinos and mediator particles in the final state. It also contains

Mixing angle	Coupling constant	Cross section (fb)	Decay Width (GeV)	$\tau^+\nu_e$
0	$g'_R = 0, g'_L = 0.64$	11.2	10.7	0.09
15	$g'_R = 0.16, g'_L = 0.62$	9.97	10.7	0.09
30	$g'_R = 0.32, g'_L = 0.56$	7.3	10.9	0.09
45	$g'_R = 0.45, g'_L = 0.45$	5.7	10.6	0.09
60	$g'_R = 0.56, g'_L = 0.32$	7.8	10.9	0.09
90	$g'_R = 0.64, g'_L = 0$	11.3	10.7	0

TABLE II: The cross section and decay width for $m'_{W'} = 350$ GeV for different mixing angles and branching ratios in $\tau\nu_\tau$ final state

spin information and can do simulations for the angular distribution of decay products. The ratio of decay in one channel divided by the total decay width is referring as the branching ratio. This is given by TAUOLA package and listed in table III Branching ratios of W' for different signal channels. table.caption.13 and is shown in fig. 4 Branching ratios of W' decays figure.caption.12 for different masses and different decay channels. All the signal processes are produced with MadGraph5 2.3.3 [24]. The output of both these packages in Les Houches Event Format (LHEF) is used by PYTHIA 8.1.5.3 [28] for partonic showering, gluon radiation, fragmentation and hadronization. Tauola package [25] used for two Tau decay process in simulation. The Tau decay width can be separated due to its narrow decay width. This package simulates both the decay of Tau in leptonic and hadronic decay.

C. Selection efficiency

The events are generated by MadGraph and τ decay is performed by Tauola package. Now we will obtain the selection efficiencies for different masses of W' at different coupling constants. For signal selection efficiency cuts as reference [6] have been used to find the selection cuts for the probability to pass for any given signal region. Efficiency cuts are reported in this paper for events reconstructed properties and these cuts are the functions of generator-level values for that property. The detector's effects are taken into account. All efficiency cuts are multiplied for different signals regions and different channels to get full selection efficiency.

The efficiency for different channels are calculated for different masses of W' bosons by running simulation code. The table IV Efficiencies of different channels for different masses in the standard

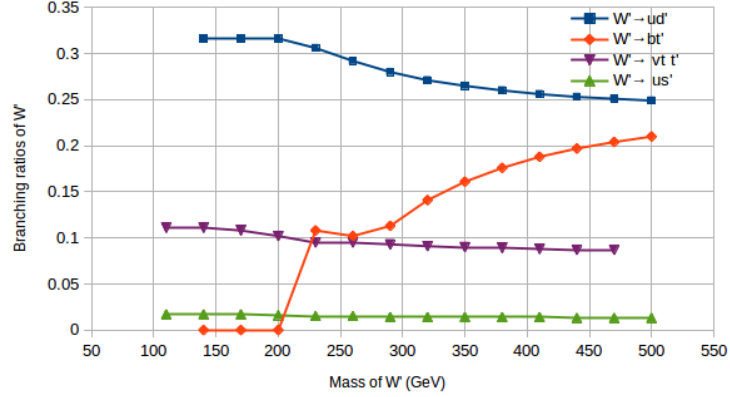


FIG. 4: Branching ratios of W' decays

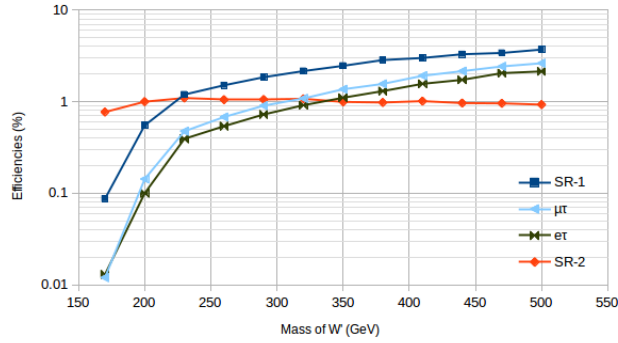


FIG. 5: Mass versus efficiency for different channels in the standard model like scenario

model like scenario table.caption.15 gives the efficiency for different channels and different masses in the standard model like scenario as shown in fig. 5 Mass versus efficiency for different channels in the standard model like scenario figure.caption.17. The efficiencies are calculated for different masses of W' and for different coupling constants (mixing angles). These results are compared with the given table IVEfficiencies of different channels for different masses in the standard model like scenario table.caption.15 and fig. 5 Mass versus efficiency for different channels in the standard model like scenario figure.caption.17 is produced in standard model like scenario, and found that

Mass (GeV)	Branching ratios ($W' \rightarrow x + y$)							
	$u + d'$	$c + s'$	$b + t'$	$e + e$	$\mu + \mu$	$\tau + \tau'$	$u + s'$	$c + d'$
110	0.32	0.32	0	0.11	0.11	0.11	0.02	0.02
140	0.32	0.32	0	0.11	0.11	0.11	0.02	0.02
170	0.32	0.32	0	0.11	0.11	0.11	0.02	0.02
200	0.31	0.31	0.03	0.11	0.108	0.11	0.02	0.02
230	0.29	0.29	0.08	0.10	0.10	0.10	0.02	0.02
260	0.28	0.28	0.11	0.10	0.10	0.10	0.02	0.01
290	0.27	0.27	0.14	0.10	0.10	0.10	0.01	0.01
320	0.26	0.26	0.16	0.09	0.09	0.09	0.01	0.01
350	0.26	0.26	0.18	0.09	0.09	0.09	0.01	0.01
380	0.26	0.26	0.19	0.09	0.09	0.09	0.01	0.01
410	0.25	0.25	0.11	0.09	0.09	0.09	0.01	0.01
440	0.25	0.25	0.20	0.09	0.09	0.09	0.01	0.01
470	0.25	0.25	0.21	0.09	0.09	0.09	0.01	0.01
500	0.24	0.25	0.22	0.09	0.09	0.09	0.01	0.01

TABLE III: Branching ratios of W' for different signal channels.

the efficiency do not depend upon the coupling strength as expected. The efficiency of the signal region is only the function of kinematics of the event generated which changes with mass of W' .

For any given integrated luminosity, the total number of expected events can be estimated in that channel, if one knows the production cross-section of the event and branching ratio (BR) of the signal and for that channel full selection efficiency by the following equation.

$$N = \mathcal{L} \times \sigma(pp \rightarrow W'^+W'^-) \times BR(W' \rightarrow \tau\nu) \times BR(W' \rightarrow \tau\nu) \times \epsilon^{ch} \quad (4)$$

Where ϵ^{ch} is the full selection efficiency. The systematic uncertainty and integrated luminosity are given in the table V Integrated luminosity and uncertainty of the channel stable.caption.16 taken from the experimental paper followed.

The number of expected events are calculated using above formula for production cross section for the standard model scenario and branching ratios of the signal of our interest ($W' \rightarrow \tau\nu$) using luminosity of the above table taken from experimental paper and the channel efficiencies listed in table VI The expected number of Events in Standard Model scenario table.caption.18 are calculated using our simulation codes.

Mass (GeV)	SR-1	SR-2	$\mu\tau$	$e\tau$
110	0.09	0.77	0.12	0.01
140	0.27	0.92	0.40	0.03
170	0.09	0.77	0.01	0.01
200	0.55	1.00	0.14	0.10
230	1.20	1.10	0.48	0.39
260	1.51	1.05	0.68	0.54
290	1.85	1.05	0.90	0.72
320	2.16	1.07	1.08	0.92
350	2.46	0.99	1.37	1.10
380	2.85	0.98	1.56	1.30
410	3.00	1.01	1.92	1.57
440	3.29	0.96	2.15	1.73
470	3.40	0.96	2.42	2.05
500	3.70	0.83	2.63	2.14

TABLE IV: Efficiencies of different channels for different masses in the standard model like scenario

Channel	Integrated luminosity(fb^{-1})	Uncertainty (%)
$\tau_h \tau_h$	18.1	20
Lepton τ_h	19.6	25

TABLE V: Integrated luminosity and uncertainty of the channels

D. Transverse mass

The detector can detect the transverse component indirectly, although detector cannot directly detect the emerging neutrinos. According to the momentum conservation the final state should not have any transverse component, because the initial transferable components of momentum are zero. When all transverse components are added and their sum is other than zero, the additional transverse component to make zero is known as missing transverse energy (MET). This energy represents neutrinos which are the only particle in the Standard Model which contribute to the missing energy. The signal missing transverse energy of the event is not because of instrumental MET but related to the real physical contents. If we do not have the invariant mass, the transverse

Mass (GeV)	σ (fb)	Luminosity		Luminosity		Γ	Expected number of Events in different signal regions			
		$\mathcal{L} = 18.1 fb^{-1}$		$\mathcal{L} = 19.6 fb^{-1}$			SR-1	SR-2	$\mu \tau$	$e \tau$
		SR-1	SR-2	$\mu \tau$	$e \tau$		SR-1	SR-2	$\mu \tau$	$e \tau$
110	2055.28	0.06	0.52	0.01	0.01	0.11	27	234	4.8	4.8
140	923.55	0.20	0.64	0.03	0.03	0.11	40.45	129.45	6.57	6.57
170	360.11	0.46	0.76	0.11	0.09	0.11	36.28	59.93	9.40	7.68
200	173.94	0.75	0.81	0.24	0.12	0.10	23.61	25.50	8.18	4.09
230	87.60	1.06	0.89	0.38	0.31	0.10	16.80	14.11	6.52	5.32
260	48.09	1.41	0.89	0.62	0.48	0.10	12.40	7.82	5.90	4.57
290	28.08	1.67	0.88	0.98	0.70	0.09	6.87	3.62	4.37	3.12
320	17.41	1.98	0.90	1.06	0.82	0.09	5.05	2.30	2.92	2.26
350	11.21	2.29	0.93	1.32	1.11	0.09	3.76	1.53	2.35	1.97
380	7.50	2.60	0.94	1.53	1.21	0.09	2.86	1.03	1.82	1.44
410	5.16	2.92	0.88	1.76	1.50	0.09	2.21	0.66	0.15	0.14
440	3.64	3.13	0.91	2.03	1.69	0.09	1.67	0.48	1.17	0.97
470	2.61	3.36	0.92	2.28	1.92	0.09	1.28	0.35	0.94	0.79
500	1.91	3.57	0.84	2.54	2.19	0.09	1.00	0.24	0.77	0.66

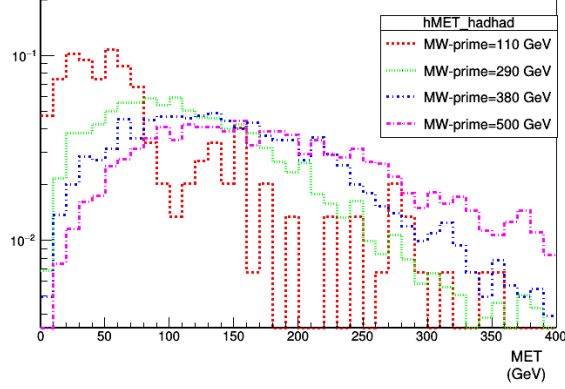
TABLE VI: The expected number of Events in Standard Model scenario

component may be reconstructed for neutrino. This is known to be called as transverse mass (M_T) rather be calculated as:

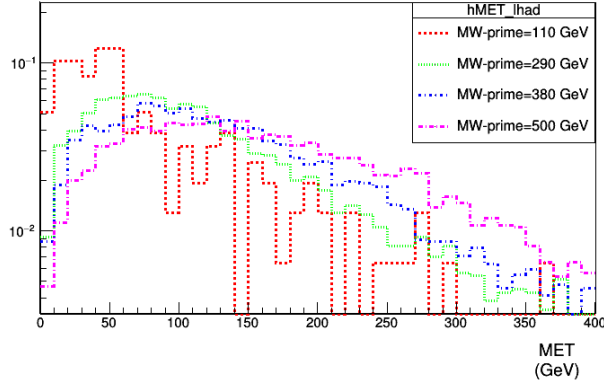
$$M_T = \sqrt{2P_T^\tau P_T^\nu (1 - \cos \Delta\theta_{\tau,\nu})} \quad (5)$$

Equation 5equation.3.5 represents the transverse momentum of τ , the missing transverse energy which is the transverse component of neutrino.

For the generated events, this was done as a cross check, and kinematics are produced. In the final state of our signal contain mixture of hadronic, leptonic and also pure hadronic channels. For different mass of W' the distribution of missing transverse momentum (P_T^{miss}) and transverse mass M_{T2} are given in figs. 6The missing transverse energy distribution is shown for a) fully hadronic and b) semi-leptnic channelfigure.caption.20(a), 6The missing transverse energy distribution is shown for a) fully hadronic and b) semi-leptnic channelfigure.caption.20(b), 7 M_{T2} distribution in for different mass of W' in different channelsfigure.caption.21(a) and 7 M_{T2} distribution in for different mass of W' in different channelsfigure.caption.21(b) for different channels.



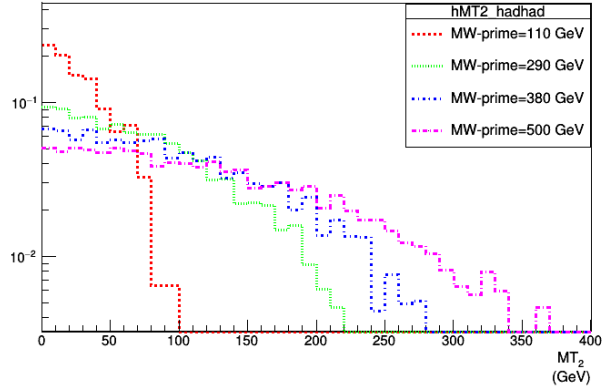
(a)



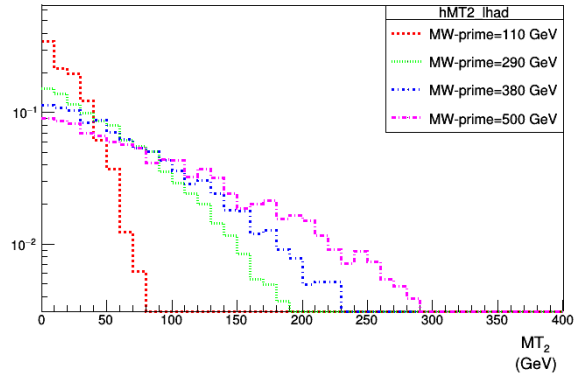
(b)

FIG. 6: The missing transverse energy distribution is shown for a) fully hadronic and b) semi-leptonic channel

The distribution of transverse momentum are given in fig. 8 Transverse momentum distributions in different channels figure.caption.22(a) and 8 Transverse momentum distributions in different channels figure.caption.22(b) of the τ_h lepton in $l\tau_h$ channels. Looking into the plot of the distribution of these variables, it is observed that heavier objects are produced with increasing mass of W' bosons. The transverse gives Jacobean's peak characteristics instead of Breit Weigner which in case of invariant mass the peak rise upto $M_T = M_{W'}$ with transverse mass and then start falling rapidly. For the statistical analysis transverse distribution is very useful.



(a)

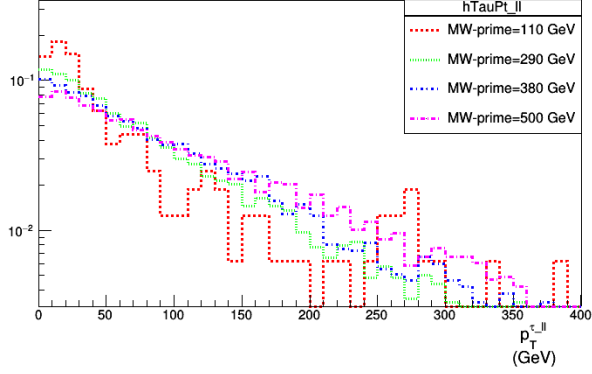


(b)

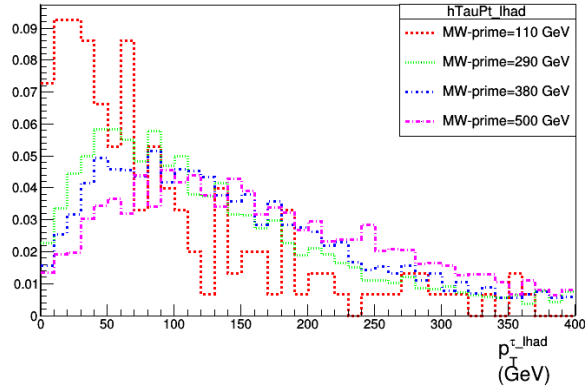
FIG. 7: M_{T2} distribution in for different mass of W' in different channels

E. Background Events

Background events are additional interactions that originate in pp collision and are mainly studied in two categories. In one class gluon and quarks jets are misidentified as τ_h and in second with genuine τ_h candidate. In the first class the dominant source are the $W+$ jets and QCD multi jets and in the second case dominated events are $Z+$ jets, Higgs bosons, di-bosons and $t\bar{t}$. Background estimations are given in detail below.



(a)



(b)

FIG. 8: Transverse momentum distributions in different channels

F. QCD Multi jets

For the $e\tau_h$ and $\mu\tau_h$ decays, it has been found that the events selected with selection cut $M_{T2} < 90$ GeV is useful to discard the SM background events. But for $\tau_h\tau_h$ events, two separate SR's are defined as events with $M_{T2} < 90$ are regarded as SR1 and events with $40 < M_{T2} < 90$ GeV and $\Sigma M_T^T > 250$ GeV are regarded as SR2, where M_T^T is the sum of the transverse mass of two τ_h objects. In signal region two hadronic jets mis-identified, appeared as a pair results into QCD multi jets production. Isolation variables are used to specify genuine and misidentified τ_h candidate. One signals region and three control region are specified for the estimation of QCD multi jets selecting threshold on search variable M_{T2} (MET) or such that $M_{T2} > 90$ GeV to 40 GeV and > 250 GeV to 100 GeV. One loose τ_h at least is selected with same sign. The non-QCD event

are subtracted based on expectation of Monte Carlo (MC) simulation. The search variables are not related, isolation misidentified candidate where QCD multi jets dominated. In the two signal regions SR-1 ($M_{T2} > 90\text{GeV}$) and SR-2 ($M_{T2} < 90\text{ GeV}$) are estimated in the table VII. QCD multi jets background table.capt.26 below.

G. $W + \text{jets}$ background

From MC simulation, $W + \text{jets}$ are zero for remaining events in channels, while due to statistical errors in simulation sample large statistical uncertainty is there. The $W + \text{background}$ contribution from simulation are taken by formula

$$N_{SR} = \epsilon_{FS} \times N_{BFS} \quad (6)$$

where

N_{SR} = $W + \text{jets}$ in signal region

N_{BFS} = before final selection ($M_{T2} > 90\text{ GeV}$ for SR-1 and $> 250\text{ GeV}$ for SR-2)

ϵ_{FS} = Final selection efficiency

The table VIII. DY background table.capt.28 gives the background with statistical uncertainty in two signal regions for $W + \text{jets}$.

Signal region	$W + \text{jets}$
SR-1	0.70 ± 0.21
SR-2	4.36 ± 1.05

TABLE VII: QCD multi jets backgrounds

H. Drell-Yan backgrounds

This background comes from MC simulation. Different lepton pairs ($ee, \tau\tau, \mu\mu$) are included in the production. Due to misidentified probability τ_h , contribution from $Z \rightarrow \tau\tau \rightarrow ll$ and $Z \rightarrow ll$ is very small for $l \rightarrow \tau_h$. For $\tau_h \rightarrow l$ misidentified probability is also very small, and the DY contribution to background from $Z \rightarrow \tau\tau \rightarrow \tau_h\tau_h$ and $Z \rightarrow \tau\tau \rightarrow l\tau_h$ are very dominant. The contribution from $Z \rightarrow \tau\tau \rightarrow \tau_h\tau_h$ very low in $l\tau_h$ channel. This is suitable in $\mu\tau_h$ control region. Table IX. Misidentified τ_h background table.capt.30 gives the estimation of DY background in $l\tau_h$ is given for genuine τ_h .

Signal region	DY-back ground
e τ_h	0.19±0.04
μ τ_h	0.25±0.06
τ_h τ_h SR-1	0.56±0.07
τ_h τ_h SR-2	0.81±0.56

TABLE VIII: DY background

I. Misidentified τ_h in $l\tau_h$ channels background

The misidentified τ_h contribution in $l\tau_h$ channels is assumed by a method in which probability of genuine isolated misidentified τ_h passes through tight isolation taken into account. The number of τ_h loose isolation candidate, when τ_h pass through loose isolation and signal selection is given by

$$N_l = N_g + N_m \quad (7)$$

Where N_l are loose, N_g are genuine and N_m are number of misidentified candidate. The number of tight candidate at tight selection as given by

$$N_t = r_m(N_t - r_g N_l / r_m - r_g) \quad (8)$$

Here r_m (r_g) gives the probability for loosely selected misidentified (genuine) τ_h that passes through tight selection. Eliminating N_g gives

$$r_m N_m = r_m(N_t - r_g N_l) / r_m - r \quad (9)$$

Contamination of misidentified τ_h is given by the product $r_m N_m$ in the signal region. The total misidentified events $l\tau_h$ channel are summarized in table XTotal backgrounds events.table.caption.31. The combined all four signal regions background are summarized in table below including Di bosons jets (vv), $t\bar{t}$ jets (tx) and higgs bosons jets (hx).

Signal region	Total Misidentified
$e \tau_h$	3.30 ± 3.35
$\mu \tau_h$	8.15 ± 4.59

TABLE IX: Misidentified τ_h backgrounds

Backgrounds	Signal Regions			
	$e \tau_h$	$\mu \tau_h$	$\tau_h \tau_h$ SR-1	$\tau_h \tau_h$ SR-2
DY	0.19 ± 0.04	0.25 ± 0.06	0.56 ± 0.07	0.81 ± 0.56
vx,vv,hx	0.03 ± 0.03	0.19 ± 0.09	0.19 ± 0.03	0.75 ± 0.35
W+ jets	3.3 ± 3.35	8.15 ± 4.59	0.70 ± 0.21	4.36 ± 1.05
QCD multi jets	0	0	0.13 ± 0.06	1.15 ± 0.39
Standard model total	3.52 ± 3.35	8.59 ± 4.59	1.58 ± 0.23	7.07 ± 1.3
Observed	3	5	1	2

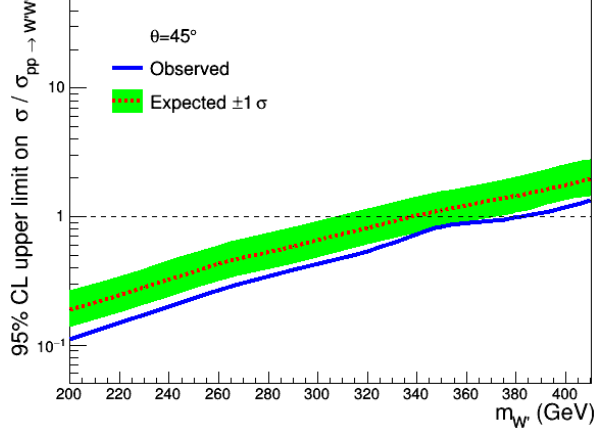
TABLE X: Total backgrounds events.

IV. EXCLUSION

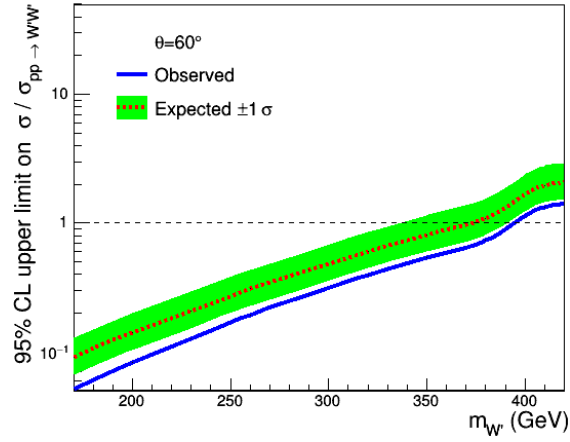
The compatibility of the observed data with the expected signals being tested can be quantitatively performed using statistical analysis. Bayesian and frequent tests are the two most famous approaches used for this compatibility test. In this study, Bayesianic approach is used to set Limit on mass of W' . This statistic based on Bayes theorem [26].

$$P(A \vee B) = \frac{P(B | A) P(A)}{P(B)} \quad (10)$$

This theorem gives the conditional probability of Event A when given B . This probability may relate to the experiment when A is considered hypothesis test. In this study, A is replaced with the new heavy gauge boson W' as a hypothesis test, while B is considered as expected results. For hypothesis (Observed data) to be true $P(A/B)$ is the probability in this theorem. To set Limits, statistical analysis is performed for which it is compulsory to choose the parameter of interest. The background events, expectation of signals and data are used to determine the probability density for this parameter. The parameter of interest selected in this study is σB , which is also a very commonly chosen parameter in different searches of W' that are published. σB is the product of cross section (σ) of signal ($pp \rightarrow W'W'$) and Branching ratio of W' decay into the required final



(a)



(b)

FIG. 9: Mass at the different mass hypothesis of W' shown when mixing angle is 45 (left) and when mixing angle is 60 (right)

stat ($W' \rightarrow \tau\nu\nu$). The limit for the mass exclusion may be calculated by comparing cross sections predicted upper limit by the theory.

Constraint on mass of W' can be set to exclude the lower mass at 95% confidence level. The signal strength is given by the ratio $\sigma / \sigma_{pp \rightarrow W'W'}$ which can be evaluated by applying the method of semi-bayesian ratio that is implemented in ROOT [27]. Different results are obtained for different cross section and efficiency to set limit on mass. The standard model like and other limits are given in the table and shown in fig. 9. Mass at the different mass hypothesis of W' shown when mixing angle is 45 (left) and when mixing angle is 60 (right) figure.captio.33. For standard model type the mass of W' upto 445 GeV are excluded. This method was repeated for different scenarios and observed that limit is proportional to coupling, that the limit increases when

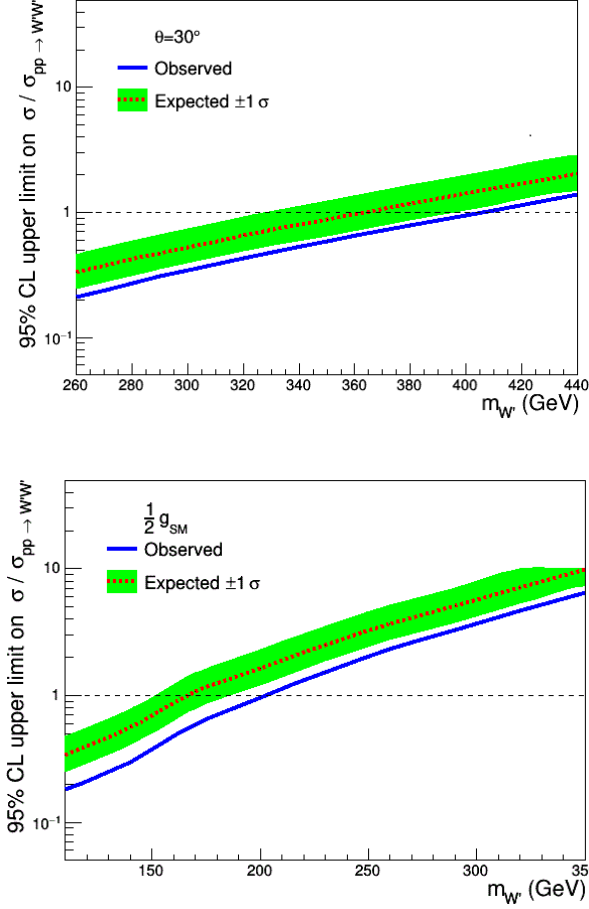


FIG. 10: The input W' masses as a function of exclusion in 95% Confidence Level

g'_L is increased and decreases when g'_L is decreased. Different observed and expected limits with uncertainty of $\pm 1\sigma$ are given in fig. 10. The input W' masses as a function of exclusion in 95% Confidence Level figure.caption.34, and table XI. The observed and expected mass limits on mass of W' table.caption.36 gives the summary of different coupling scenarios for observed and expected limits. Transverse mass distribution reconstructed from lepton pairs from each mass hypothesis assumed and is shown in fig. 11. Mass of W' assumed for different mass hypothesis, shown observed and expected limits when coupling is exactly equal to SM coupling (left) and when coupling is one and half times the SM coupling (right) figure.caption.35. As seen in table and figure that, the observed limit is always higher than the expected which could be due to the fact that large expected backgrounds in different signals region than the observed data given in the background summary table X. Total backgrounds events. table.caption.31. We observed that compared to direct searches, the results are lower but any new model can be helpful to put possible constraints having same final state using this model, with no need of real detector response to simulate.

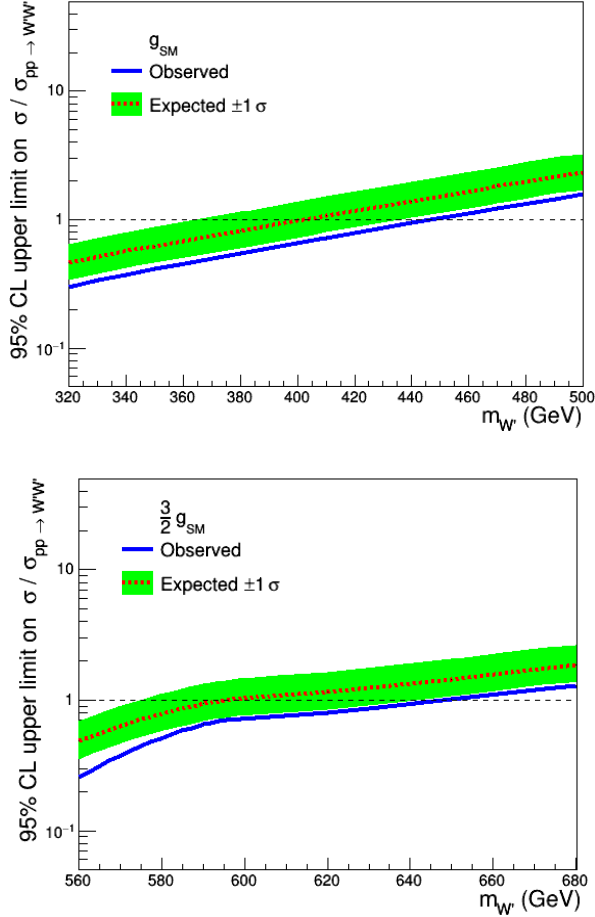


FIG. 11: Mass of W' assumed for different mass hypothesis, shown observed and expected limits when coupling is exactly equal to SM coupling (left) and when coupling is one and half times the SM coupling (right)

V. CONCLUSION

The W' pair production is easily accessible as we increase the center of mass energy for pp collision. The production cross section and the decay width are calculated for different coupling strengths and for different masses. It has been observed that with the increasing mass of W' the decay width is increasing while the production cross section is decreasing as expected. The signal region efficiencies are found invariant with coupling strength but change with mass. This shows that it only depends upon the kinematics of the process which is related to W' mass, which is increasing with W' mass. For transverse parameters (Momentum, missing energy and mass) treatment is done which gives a distribution plot of these parameters. The distribution shows that with increasing mass of W' makes it accessible to get harder objects.

Mixing scenarios	Observed	expected
SM	445	400
$\frac{1}{2} \times g_{SM}$	200	160
$\frac{3}{2} \times g_{SM}$	645	595
$\theta = 30$	405	365
$\theta = 45$	395	375
$\theta = 60$	380	340

TABLE XI: The observed and expected mass limits on mass of W'

We have used the selection efficiencies provided for the same final state by the CMS experiment rather to fill in the complex situation of simulation for full response of detectors. These efficiencies are used for the yield of favorite signals. Statistical analysis tools are used to check the observed results with the signal yields that make it easy to set a lower limit on W' mass. The lower limits for the different scenarios are reported when different coupling strengths are used. For the coupling constant same as the Standard Model, it is reported that the mass below 445 GeV at the confidence level of 95% are excluded. This exclusion limit may be raised up to 645 GeV when different coupling strengths are used.

VI. ACKNOWLEDGMENT

We gratefully acknowledge support from the Simons Foundation and member institutions. The current submitted version of manuscript is available on arXiv pre-prints home page <https://arxiv.org/pdf/2003.08558.pdf> arXiv:2003.08558.

-
- [1] Z. Sullivan, “ Fully differential W' production and decay at next-to-leading order in QCD”, Phys. Rev. D 66 075011, arXiv:hep-ph/0207290, (2002).
 - [2] M. Schmaltz, Journal of High Energy Physics 2004, 056 (2004)
 - [3] R. N. Mohapatra and J. C. Pati, Phys. Rev. D 11, 566 (1975).
 - [4] R. N. Mohapatra and J. C. Pati, Phys. Rev. D 11, 2558 (1975).
 - [5] G. Senjanovic and R. N. Mohapatra, Phys. Rev. D 12, 1502 (1975).
 - [6] M. Aaboud et al. (ATLAS) “Search for a new heavy gauge boson resonance decaying into a lepton and missing transverse momentum in 36 fb⁻¹ of pp collisions at $\sqrt{s}= 13$ TeV with

- the ATLAS experiment”, Eur. Phys. J. C 78 (2018) 401, arXiv:1706.04786, (2017).
- [7] The ATLAS Collaboration, “ Search for a heavy charged boson in events with a charged lepton and missing transverse momentum from pp collisions at $\sqrt{s}=13$ TeV with the ATLAS detector”, Phys. Rev. D 100, 052013 (2019)
- [8] V. Khachatryan et al. (CMS), ”Search for electroweak production of charginos in final states with two τ leptons in pp-collisions at $\sqrt{s}=8$ TeV”, JHEP 04, 018 (2017), 1610.04870, (2017).
- [9] The CMS Collaboration, “Search for heavy gauge W' bosons in events with an energetic lepton and large missing transverse momentum at $\sqrt{s}=13$ TeV” Phys. Lett. B 770 (2017) 278
- [10] Biplob Bhattacharjee et al., “Anatomy of Heavy Gauge Bosons in a Left-Right Supersymmetric Model”, Phys. Rev. D 100, 075010 (2019)
- [11] Fei Huang et al., “Search for W' signal in single top quark production at the LHC”, Chinese Physics C, Volume 42, Number 3, (2018).
- [12] Saeid et al., “ W' pair production in the light of CMS searches”, J. Phys. G: Nucl. Part. Phys. 45 (2018) 055004
- [13] G. Arnison et al. [UA1 Collaboration], “Further Evidence for Charged Intermediate Vector Bosons at the SPS Collider”, Phys. Lett. B 129, 273-282 (1983).
- [14] G. Arnison et al. [UA1 Collaboration], “Intermediate Vector Boson Properties at the CERN Super Proton Synchrotron Collider”, Europhys. Lett. 1, 327-345 (1986).
- [15] R. Ansari et al. [UA2 Collaboration], “Search for Exotic Processes at the CERN p \bar{p} Collider”, Phys. Lett. B 195, 613 (1987).
- [16] C. Albajar et al. [UA1 Collaboration], “Studies of Intermediate Vector Boson Production and Decay in UA1 at the CERN Proton - Antiproton Collider”, Z. Phys. C 44, 15-61 (1989).
- [17] F. Abe et al. [CDF Collaboration], “Search for Charged Bosons Heavier than the W Boson in p \bar{p} Collisions at $\sqrt{s} = 1800$ GeV”, Phys. Rev. Lett. 74, 2900 (1995).
- [18] S. Abachi et al. [D0 Collaboration], “Search for Right-Handed W Bosons and Heavy W' in p \bar{p} Collisions at $\sqrt{s} = 1.8$ TeV”, Phys. Rev. Lett. 76, 3271 (1996).
- [19] J. Alitti et al. [UA2 Collaboration], “A measurement of two-jet decays of the W and Z bosons at the CERN p \bar{p} collider”, Z. Phys. C 49, 17 (1991).
- [20] J. Alitti et al. [UA2 Collaboration], “A Search for new intermediate vector mesons and excited quarks decaying to two jets at the CERN p \bar{p} collider”, Nucl. Phys. B 400, 3-24 (1993).
- [21] F. Abe et al. [CDF Collaboration], “Search for new particles decaying to dijets at CDF”, Phys. Rev. D 55, 5263 (1997).
- [22] F. Abe et al. [CDF Collaboration], “Search for a W' Boson via the Decay Mode $W' \rightarrow \mu\nu\mu$ in 1.8 TeV p \bar{p} Collisions”, Phys. Rev. Lett. 84, 5716 (2000).
- [23] T. Affolder et al. [CDF Collaboration], “Search for Quark-Lepton Compositeness and a

- Heavy W' Boson Using the $e\nu$ Channel in $p\bar{p}$ Collisions at $\sqrt{s} = 1.8$ TeV”, *Phys. Rev. Lett.* 87, 231803 (2001).
- [24] J. Alwall, M. Herquet, F. Maltoni, O. Mattelaer, and T. Stelzer, “MadGraph 5: going beyond”, *JHEP* 06, 128 (2011), arXiv:1106.0522, (2011).
- [25] N. Davidson, G. Nanava, T. Przedzinski, E. Richter-Was, and Z. Was, “Universal Interface of TAUOLA Technical and Physics Documentation”, *Comput. Phys. Commun.* 183, 821-843, e-Print 1002.0543, (2012).
- [26] V. Blobel and E. Lohrmann. *Statistische und numerische Methoden der Datenanalyse*. Teubner-Studienb Fcher. Physik Wiesbaden, Germany: Vieweg+Teubner Verlag, 1998. ISBN 9783519032434.
- [27] R. Brun and F. Rademakers, “ROOT: An object oriented data analysis framework”, *Nucl. Instrum. Meth.* A389, 81-86 (1997).
- [28] T. Sjostrand, S. Mrenna, .and P. Skands, A Brief Introduction to PYTHIA 8.1, *Comput. Phys. Commun.* 178 (2008) 852–867, [0710.3820].
- [29] Cacciari, M., Salam, G.P., Soyez, G.: *JHEP* 04, 063 (2008). arXiv:0802.1189.